Desalination and Water Treatment
www.deswater.com

doi: 10.5004/dwt.2019.23253

138 (2019) 120–127
January

Facile synthesis of sulfur-free expanded graphite under mild conditions and its adsorption property

Dan Liu, Qinghua Mao, Yunshan Bai*, Hongzhu Ma*

Laboratory of Applied Surface and Colloid Chemistry, Ministry of Education, School of Chemistry and Chemical Engineering, Shaanxi Normal University, Xi'An, Shaanxi 710119, China; emails: ysbai@snnu.edu.cn (Y. Bai), hzmachem@snnu.edu.cn (H. Ma)

Received 17 March 2018; Accepted 6 October 2018

ABSTRACT

Under mild conditions, sulfur-free expanded graphite (SFEG) was prepared facilely, and the maximum expansion volume up to 287.8 mL/g was obtained. The effect of various operation conditions was optimized. Various characterizations demonstrated that SFEG with well-developed network pores in the wormlike particles and functional groups (C–O, C=O, C=C, O=C–O, and –COOH) has been successfully synthesized. The adsorption capacities toward gear oil and methylene blue were investigated, and the results showed that SFEG exhibited excellent adsorption capacities and selective adsorption property, which could be attributed to the functional groups and well-developed network pores in the wormlike SFEG.

Keywords: Sulfur-free; Expanded graphite; Intercalation; Adsorption capacity; Methylene blue

1. Introduction

Expanded graphite (EG) has been widely concerned and exhibited great application potential in many fields, because of its excellent properties, such as large adsorption capacity, low density, excellent chemical stability, high recycling efficiency, environment friendliness, and high porosity [1,2]. In particular, it can act as an excellent adsorbent material for the treatment of oil spills [3,4] and dye removal from wastewater [5,6]. In the preparation of EG, a series of organic and inorganic compounds have been used as intercalators, such as formic acid [7], glacial acetic acid [8], sulfuric acid [9], hydrogen peroxide [10], perchloric acid [2], and so on. Generally, sulfuric acid has been applied, thereby resulting in the residual of sulfur species in the as-fabricated samples, which limited its wide application.

So far, a variety of procedures [5,11,12] on low sulfur or sulfur-free expanded graphite (SFEG) have been studied. Generally, SFEG can be obtained by combined oxidation intercalation agent. Especially, perchloric acid and potassium permanganate are the most commonly used [8,5,11–14], following by thermal treatment at higher temperature or electrochemical treatment with electrolyte employed. At the same time, a large amount of oxidized intercalations are also needed and used in the preparation process, which increased the burden on the environment. Therefore, it is necessary to develop mild and environmentally friendly method by which SFEG can be prepared.

In this work, natural flake graphite (NFG) was oxidized by $KMnO_4$–HNO_3–citric acid (CA) trinary system under mild conditions, followed by microwave. In comparison with the conventional chemical oxidation method for EG preparation, the potassium permanganate and nitric acid oxidant system was also utilized, while CA as a mild organic acid was firstly used as an assisted intercalation agent. The effect of various operation conditions for synthesis of SFEG was investigated and optimized. The resulting SFEG was characterized by scanning electron microscopy (SEM), X-ray diffraction (XRD), Fourier-transform infrared spectroscopy (FTIR), Raman spectroscopy, X-ray photoelectron spectroscopy (XPS), and nitrogen adsorption apparatus. Textile wastewater effluents and oil leakage result in serious environmental pollution; it is urgent and necessary to remove these pollutants from

* Corresponding authors.

wastewater [15,16]. Here, gear oil and methylene blue (MB) were selected as the model pollutants, and the adsorption capacities of SFEG were studied.

2. Materials and methods

2.1. Materials

The NFG with an average size of 35–48 mesh was applied. CA ($C_6H_8O_7{\cdot}H_2O$), $KMnO_4$, and HNO_3 (65.0–68.0 wt.%) in analytical purity were purchased from Sinopharm Chemical Reagent Co., Ltd., Shanghai, China; gear oil was obtained from Lankun Lubricating Oil Co., Ltd., Lanzhou, China. MB in analytical purity was purchased from Northwest Institute of Non-ferrous Geology, Xi'an, China.

2.2. Preparation of SFEG

The graphite intercalation compound (GIC) was prepared by a conventional chemical oxidation process as follows [13]: NFG (0.5 g) was mixed with a certain amount of HNO_3 (6.0–8.5 mL) and $KMnO_4$ (0.03–0.08 g) in a water bath at 35°C for 80 min for oxidizing the graphite layer and intercation with continuous stirring at 50 rpm. Herein, HNO_3 was served as oxidant and inserting agent, while $KMnO_4$ as oxidant. Then as an auxiliary intercalant, CA (0–0.45 g) was introduced with continue stirring at 50 rpm for 20 min for further intercation. Then the residue was collected and washed with distilled water for several times till pH 7, dried for 12 h in a vacuum oven at 60°C, to obtain GIC for further use.

The obtained GIC sample was placed in a quartz culture dish in microwave oven (WD900ASL23-2, Shunde Galanz Electric Appliance Industry Co., Ltd., Guangdong, China) was further expanded at 180 W for several seconds, a worm-like SFEG was obtained, as shown in Fig. 1.

According to the National Standard of China (GB 10698-1989), the expanded volume (EV) of SFEG was measured: the synthesized samples were gently transferred into a 100 mL graduated cylinder, and the volume (V) occupied and mass (M) of SFEG were recorded. The EV (mL/g) was calculated by Eq. (1) [14]:

$$EV = \frac{V}{M} \tag{1}$$

2.3. Characterization

The morphologies and chemical composition of the as-prepared samples were studied recorded by SEM (Quanta 200, FEI, Hillsborough, USA), Powder XRD (D8Advance, Germany), FTIR (Bruker, Germany), Raman spectroscopy (Raman Spectrometer, in Via Reflex, Britain), and XPS (AXIS ULTRA, Japan). Nitrogen adsorption–desorption isotherms were obtained on a nitrogen adsorption apparatus (ASAP2020/HD88, Mike instruments Inc., USA).

2.4. Adsorption capacity

The adsorption performance of the as-prepared SFEG sample was evaluated by the adsorption of MB and gear oil.

The adsorption of MB was performed at 35°C under alkaline conditions (pH = 11.76) [17]. In each run, 0.030 g SFEG adsorbent was added into 10 mL MB of 50 mg/L with stirring at 250 rpm. At the given time intervals, SFEG sample was separated by centrifugation and the residue concentration of MB in solution were measured at the maximum wavelength (λ_{max} = 664.2 nm) with an ultraviolet–visible spectrophotometer (Beijing Purkinje General instrument Co., Ltd.). Herein, the MB removal (R%) was calculated based on the MB concentration before and after adsorption according to Eq. (2) [18]:

$$R\% = \left(\frac{c_0 - c_t}{c_0}\right) \times 100\% \tag{2}$$

where c_0 is the initial concentration of MB, and c_t is concentration of MB at time t. Each experiment was duplicated thrice under identical conditions to confirm the reproducibility of the experiments.

Gear oil as the oil candidate was selected as the target pollutant to evaluate the selective adsorption capacity of SFEG for the potential application in crude oil leakage treatment. At room temperature, 0.15 g SFEG was immersed in a binary simulated system consisted of 8 mL gear oil and 20 mL of water to evaluate the selective adsorption capacity of SFEG adsorbent.

3. Results and discussion

3.1. Optimization of the various preparation parameters of SFEG

The adsorption capacity of SFEG was closely related to the degree of expansion, the influence of various preparation parameters such as the amount of oxidants and intercalants, oxidation temperature, and time on the EV values were systematically studied, and the results are presented in Fig. 2.

Fig. 2(a) shows that the EV increased with increase of $KMnO_4$ dosage, and the maximum EV value of 287.8 mL/g was obtained with 0.06 g $KMnO_4$. It may be because the amount of oxidant was not enough to open thoroughly the graphite layers when the amount of $KMnO_4$ was lower than 0.06 g.

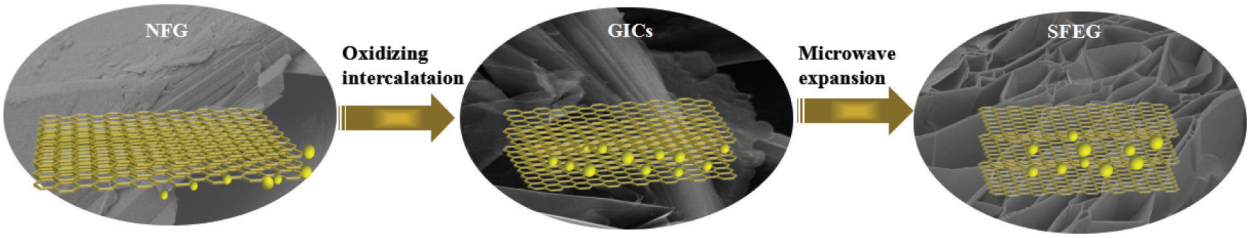

Fig. 1. Illustration of the whole synthesis process.

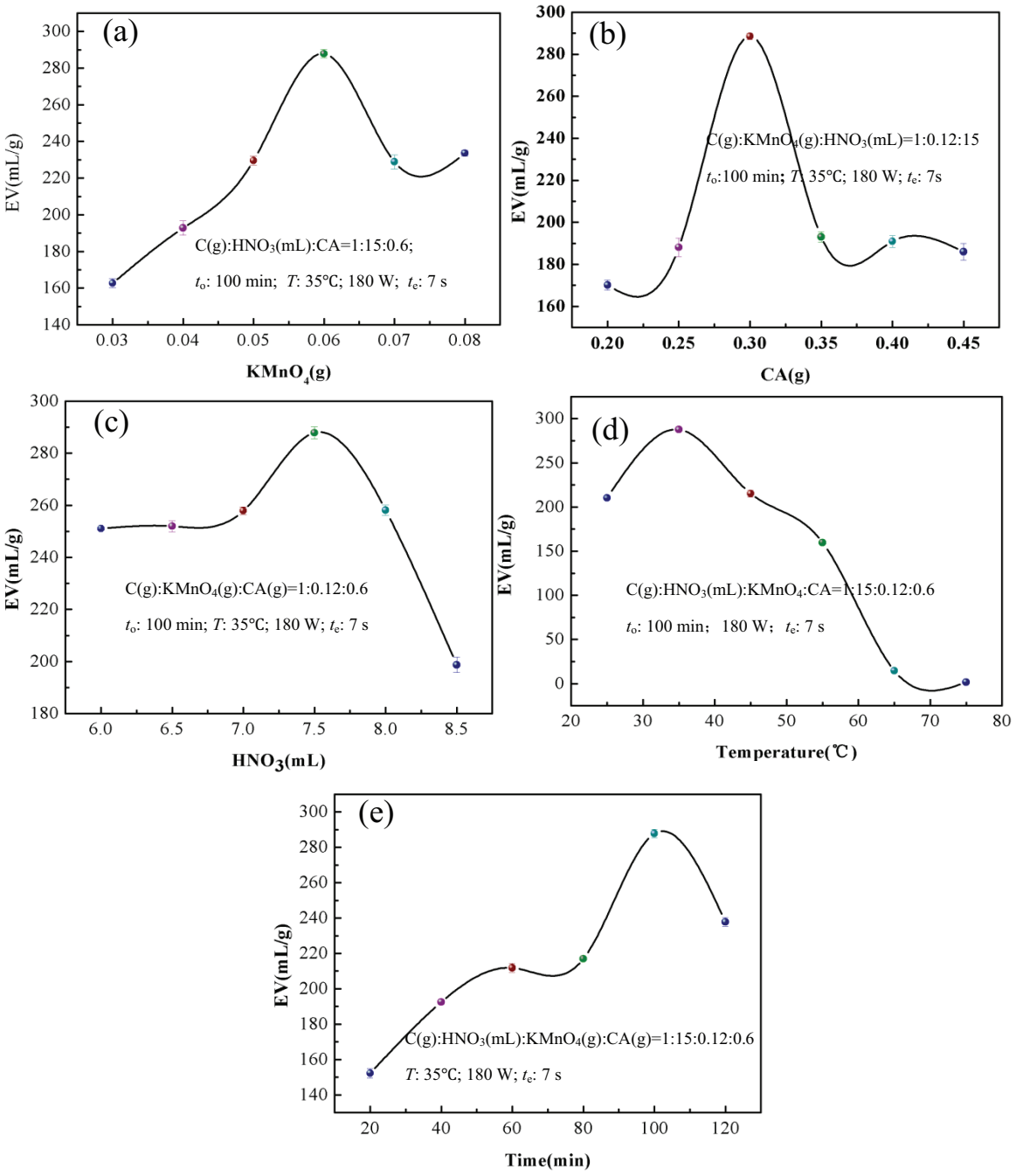

Fig. 2. Optimization of preparation parameters of SFEG.

When $KMnO_4$ dosage was further increased, the EV values significantly decreased. The EV values decreased for amount of $KMnO_4$ higher than 0.06 g, maybe due to the oxidation of NFG was excessive or the increase of distance of interlamination was so large that the inserting species escaped from there [19].

CA is an important organic acid with large polarity and soluble in water, limited researches were reported on EG synthesis with CA as the intercalant. It was found that the EV value increased with CA dosage increasing as shown in Fig. 2(b). When CA dosage was 0.3 g, the maximum EV value of 287.8 mL/g was achieved. At dosage lower than 0.3 g, CA was oxidized by $KMnO_4$ before it could be entered into the interlayer of NFG, while higher amount of CA consumed more oxidants, so 0.3 g CA was applied in the further study.

In this system, HNO_3 can act as both oxidant and intercalant. When the amount of HNO_3 was lower than 7.5 mL (Fig. 2(c)), EV values increased with HNO_3 increasing, maybe due to the oxidation intercalation reaction was incomplete at lower oxidant dosage. When the dosage of HNO_3 increased higher than 7.5 mL, EV values decreased sharply. Therefore, the optimum amount of HNO_3 for the preparation of SFEG was 7.5 mL.

It is known that the temperature has an important impact on the degree of oxidation. At lower temperature, the intercalation was insufficient and lower EV values were observed (Fig. 2(d)). The EV value reached the maximum when the temperature was up to 35°C, then decreased with temperature further increased. This might be due to, on one hand, the intercalation reaction was exothermic that was unfavorable at higher temperature. On the other hand, part of the intercalant and the oxidant was volatilized at higher temperature. So, the follow-up experiment was carried out at 35°C.

The EV values gradually increased with the time of oxidation reaction prolonging, and the maximum EV value of 287.8 mL/g was achieved at 100 min, then gradually decreased (Fig. 2(e)), may be due to the oxidant and the intercalant gradually consumed as the reaction proceeded.

From the above discussions, it could be concluded that at the optimal operation conditions—NFG: 0.5 g; $KMnO_4$: 0.06 g; HNO_3: 7.5 mL; CA: 0.3 g at 35°C for 100 min, then further expanded at 180 W for several seconds—the maximum EV of SFEG of 287.8 mL/g was obtained.

3.2. Characterization of the prepared EG

3.2.1. SEM analysis

Fig. 3 shows SEM images of various graphite samples. The lamellar structure with lateral dimensions of several micrometers and small layer distances was observed for NFG (Fig. 3(a)). After oxidation and intercalation, the surface of GIC (Fig. 3(b)) was rougher, while the interlayer was opened faintly. After microwave expanded at 180 W for several seconds, the layer distances enlarged significantly and a vermiform in shape with loose and porous structure for SFEG was observed (Fig. 3(c)). The expansion of the graphite in the direction of the *c*-axis [20] contributed to the formation of SFEG, which corresponds well to the change of *d* value confirmed by XRD analysis.

3.2.2. XRD analysis

In the XRD patterns (Fig. 4), the diffraction peaks at $2\theta = 26.381°$ ($d_{002} = 3.3756$ Å), which assigned to the normal

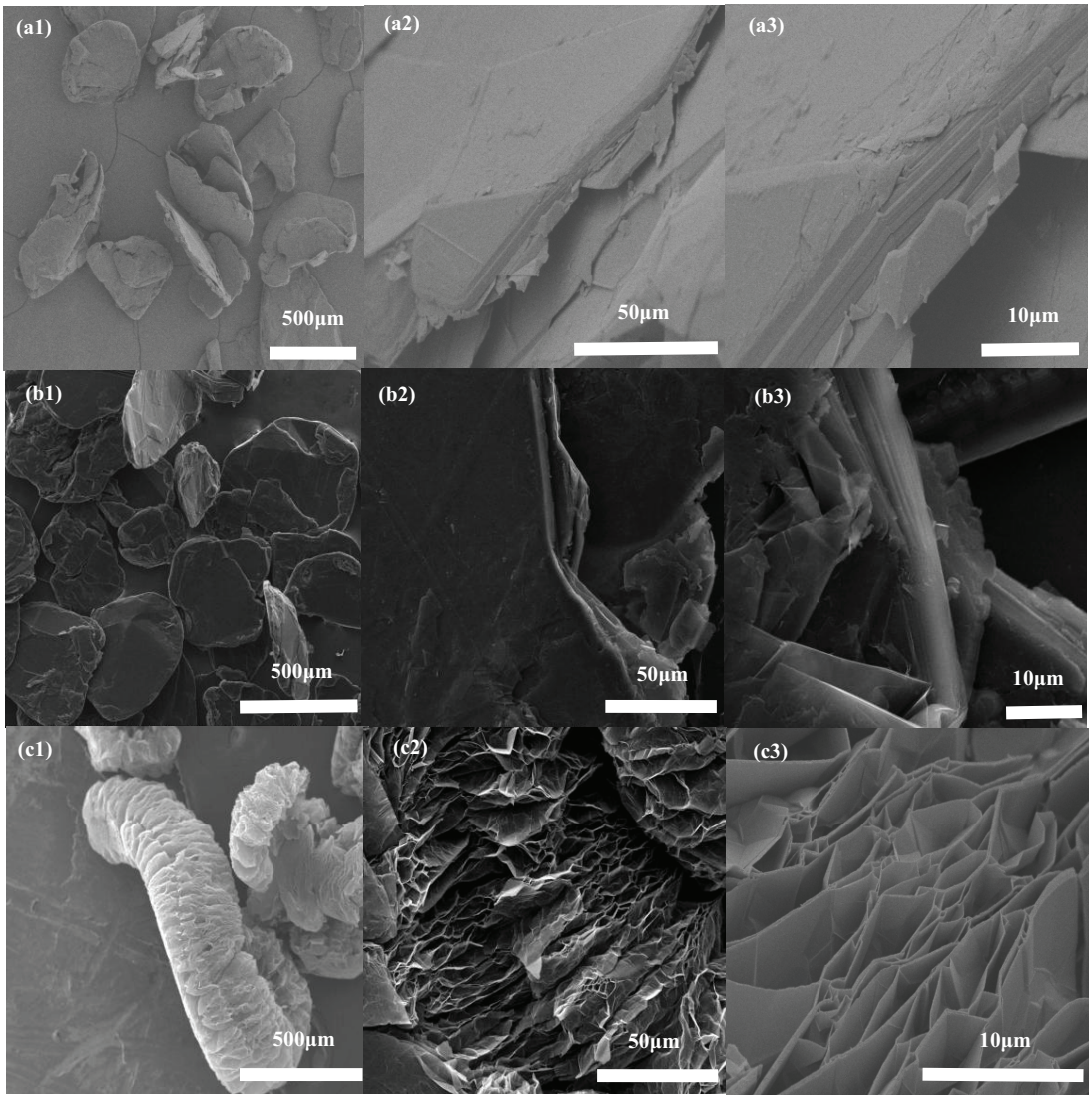

Fig. 3. SEM images of (a) NFG, (b) GIC, and (c) SFEG.

graphite spacing (002) of graphite plane [21]. In a proper oxidizing system, surface or edge of graphite plane was oxidized without destroying the layer structure. Due to conjugate system, positive charge would be dispersed onto carbon atoms in one layer, and the surface of graphite could be further oxidized and the intercalators can thus easily intercalate into graphite [20,21]. In the XRD pattern of GIC (PDF#26-1080), d_{002} = 3.3480 Å was obtained (2θ = 26.603°), which changed the original graphite dense layers structure. After microwave expansion, the SFEG (PDF#41-1487) (a) interlayer compound has changed the peak position and interplanar spacing of 2θ = 26.381 (d_{002} = 3.3756 Å), was observed. The *d* value is slightly lower than GICs *d* value. The SFEG obtained by being treated with the mixture of CA and concentrated nitric acid exhibited good flexibility in this experiment, and the interlayer can be opened with a trace of oxidant. As shown in the SEM image of the EG, the furrows structure resulting from the parting of packed layers can provide channels to facilitate the transport of adsorbate. So it is expected that the EG might have a fast adsorption rate.

3.2.3. FTIR analysis

Fig. 5 shows FTIR spectra of various graphites. The broad absorption band at 3,444 cm^{-1} assigned to the O–H stretching vibration. The peaks at 2,979 and 2,880 cm^{-1} ascribed to the –CH stretching vibration [22]. Two bands at 2,360 and 2,340 cm^{-1} assigns assigned to CO_2 stretching vibration [23].

During intercalation of natural graphite by strong acids, some of the carbon double bonds were oxidized, which led to the formation of oxygen-containing functional (carboxylic and carbon–oxygen bond) groups on exfoliated graphite surface [9]. The peak at 2,358 cm^{-1} assigned to COO^- vibration [24]. At the same time, two new peaks at 1,046 and 1,226 cm^{-1} assigned to C–O stretching vibration in CA [25,26]. N–H out-of-plane and in-plane bending were observed at 880 cm^{-1} [27], indicating that the intercalation agent nitric acid was successfully inserted into the graphite layer. The surface polar groups of the adsorbents favor the adsorption of the cationic dye.

3.2.4. Raman analysis

Raman spectroscopy is a powerful non-destructive technique to characterize the ordered and disordered structure of the graphite [5]. Fig. 6 shows the Raman spectra of SFEG and NFG. The G peak at 1,578 cm^{-1} arose from the sp^2 vibration of carbon atoms in a two-dimensional hexagonal lattice [9,28]. The D peak at 1,356 cm^{-1} was ascribed to the sp^3 vibration of carbon atoms of defects and disorders caused by the intercalation of strong acid into the graphite layers during the SFEG preparation process [29]. The intensity ratio of D and G bands (I_D/I_G) could be used to evaluate the structural damage and chemical changes of graphite [30]. The higher the I_D/I_G ratio, the lower the degree of order. The I_D/I_G ratios were 0.522 and 0.2077 for SFEG and NFG, respectively, suggesting that more structural defects were formed during the expansion process.

3.2.5. Analysis of BET and pore structure

Specific surface areas and pore volumes for NFG, GIC, and SFEG samples are summarized in Table 1. SFEG sample exhibited the highest specific surface area (34.1 m^2/g) and microporous structure, indicating that the adsorption performance should be enhanced [31].

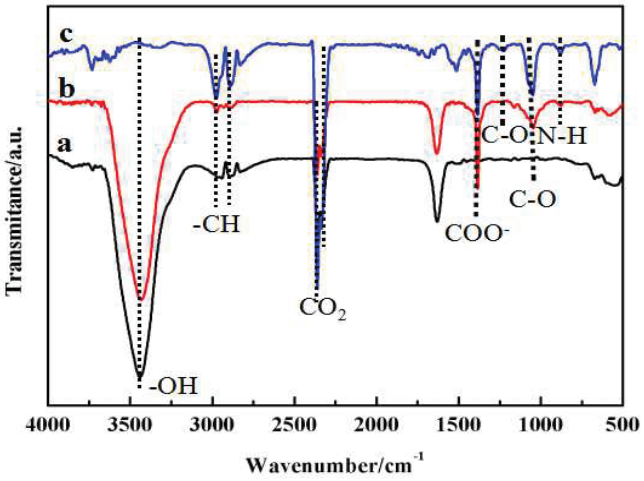

Fig. 5. FTIR spectra of (a) GIC, (b) SFEG, and (c) NFG.

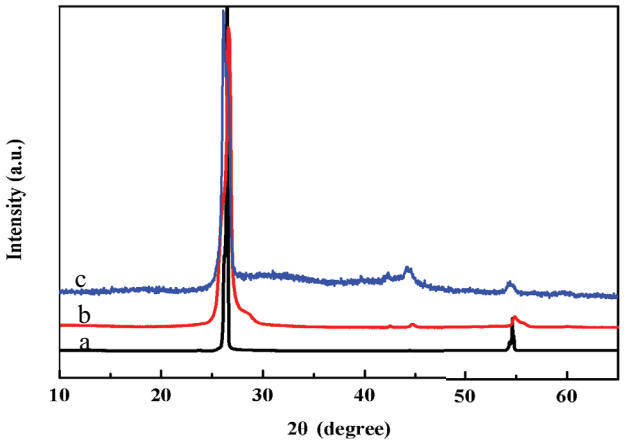

Fig. 4. XRD patterns of (a) SFEG, (b) GIC, and (c) NFG.

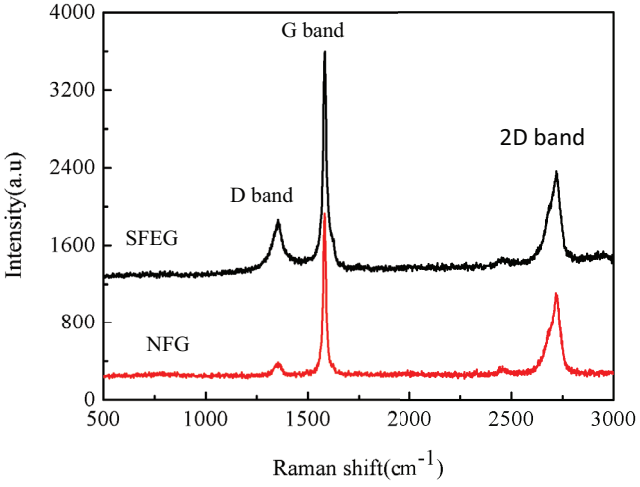

Fig. 6. Raman spectra of SFEG and NFG.

Table 1
Specific surface areas and pore volumes for NFG, GIC, and SFEG samples

Samples	BET surface area (m^2/g)	Total pore volume (mL/g)	Average pore size (nm)
NFG	0.3	–	–
GIC	4.5	–	6.2
SFEG	34.1	0.13	15.8

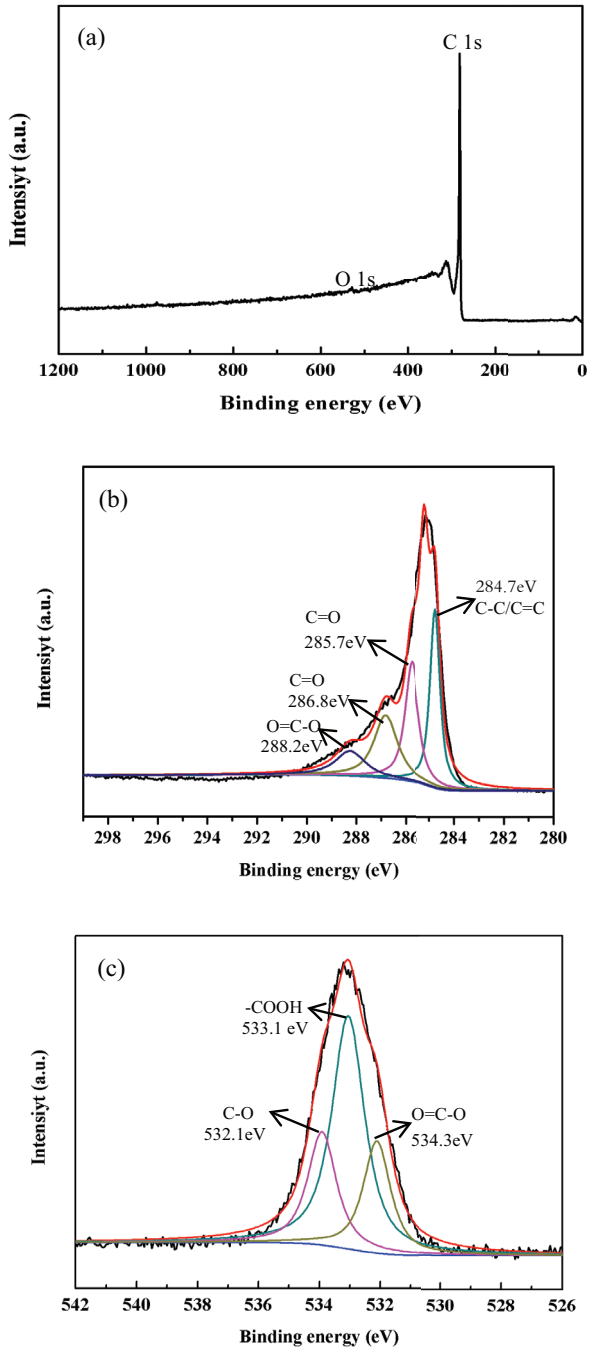

Fig. 7. (a) XPS of SFEG, (b) the spectra of C 1s, and (c) the spectra of O 1s.

3.2.6. XPS analysis

XPS technique is used to identify the surface elemental compositions and the chemical state of the materials. From Fig. 7(a), carbon oxygen elements were detected in SFEG. The survey spectra of C 1s in Fig. 7(b) indicate that the main signals at binding energies of 288.2, 286.8, 285.7, and 284.7 eV are assigned to O=C–C, C=O, C–O, and C–C/C=C species, respectively [32]. In addition, it can be clearly seen from the O 1s spectra of SFEG (Fig. 7(c)) can be deconvoluted into three peak component with binding energy of 532.1, 533.7, and 534.3 eV, attributed to the O–H [33], –COOH [34], and O=C–O [35] functional groups, respectively. These results suggested that some functional groups, such as C–O, C=O, C=C, O=C–O, O=C–C, and –COOH, were produced during the oxidation and expanded process

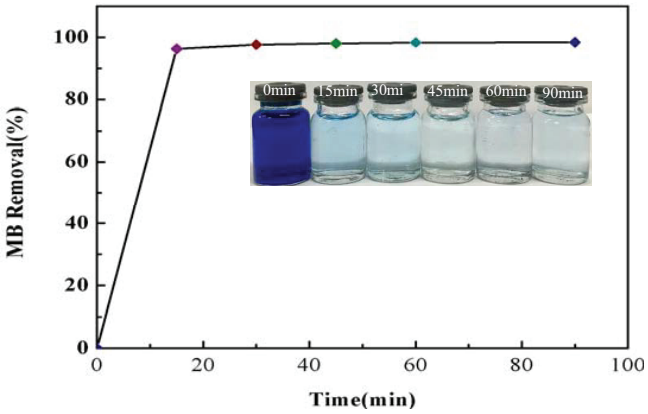

Fig. 8. The adsorption of SFEG toward MB under alkaline condition (0.030 g SFEG, 10 mL 50 mg/L MB, pH = 11.76).

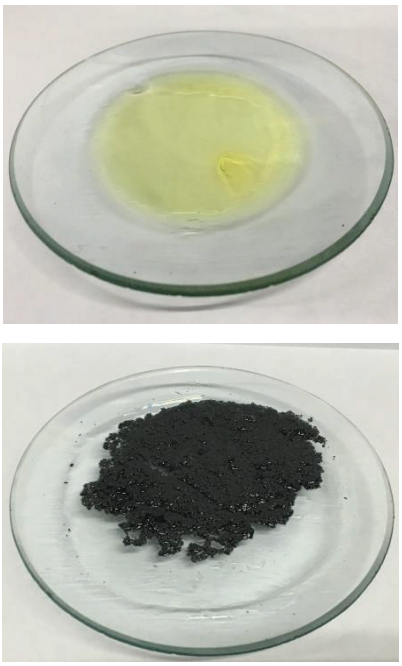

Fig. 9. Selective adsorption property of SFEG toward gear oil.

3.3. Adsorption properties

3.3.1. Dye adsorption

Clearly, it can be seen that MB removal under alkaline conditions (pH = 11.76) significantly increased with the contact time prolonged (Fig. 8). Under alkaline conditions, the produced carboxyl groups in $–COO^-$ form offer the impetus for interact of SFEG adsorbent with MB, and were benefit for adsorption process [17]. Particularly, it should be noted that the equilibrium for adsorption of MB onto SFEG took only 30 min, suggesting that SFEG exhibited higher adsorption capacity toward the contaminants. The excellent adsorption capacity should be attributed to the oxygen-containing functional groups and well-developed network pores in the wormlike SFEG [36].

3.3.2. Selective adsorption property of SFEG toward oil

For oil sorption, it was astonished to find that the gear oil in the oil-water binary system was adsorbed quickly and entirely within 2 min (Fig. 9), indicating its excellent selective adsorption capacity toward lipophilicity pollutants and potential application on crude oil leakage.

4. Conclusions

SFEG with large EV was successfully prepared under mild conditions: NFG: 1 g, $KMnO_4$: 0.12 g, CA: 0.3 g, HNO_3: 15 mL, at 35°C for 100 min for the oxidation and intercalation, followed by microwave power 180 W for several seconds for further expansion, the maximum EV of SFEG up to 287.8 mL/g was obtained. Well-developed network pores in the wormlike particles of SFEG was clearly observed. Some functional groups such as C–O, C=O, C=C, O=C–O, O=C–C, and –COOH yielded confirmed by XPS analysis. This study provided a new strategy to prepare EG under mild conditions. In addition, SFEG exhibited excellent adsorption capacity toward MB and gear oil, which attributed to the functional groups and well-developed network pores in the wormlike SFEG, suggesting its potential applications in dye textile wastewater and crude oil leakage treatment.

References

[1] G.L. Wang, Q.R. Sun, Y.Q. Zhang, F.J. Fan, L.M. Ma, Sorption and regeneration of magnetic exfoliated graphite as a new sorbent for oil pollution, Desalination, 263 (2010) 183–188.
[2] N. Sykam, K.K. Kar, Rapid synthesis of exfoliated graphite by microwave irradiation and oil sorption studies, Mater. Lett., 117 (2014) 150–152.
[3] M. Totoda, M. Inagaki, Heavy oil sorption using exfoliated graphite: new application of exfoliated graphite to protect heavy oil pollution, Carbon, 38 (2000) 199–210.
[4] B. Tryba, J. Przepiorski, A.W. Morawski, Influence of chemically prepared H_2SO_4-graphite intercalation compound (GIC) precursor on parameters of exfoliated graphite (EG) for oil sorption from water, Carbon, 41 (2003) 2013–2016.
[5] X.J. Yu, J. Wu, Q. Zhao, X.W. Cheng, Preparation and characterization of sulfur-free exfoliated graphite with large exfoliated volume, Mater. Lett., 73 (2012) 11–13.
[6] M. Zhao, P. Liu, Adsorption of methylene blue from aqueous solutions by modified expanded graphite powder, Desalination, 249 (2009) 331–336.
[7] F. Kang, Y. Leng, T.Y. Zhang, Electrochemical synthesis and characterization of formic acid-graphite intercalation compound, Carbon, 35 (1997) 1089–1096.
[8] J.H. Li, H.F. Da, Q. Liu, S.F. Liu, Preparation of sulfur-free expanded graphite with 320 μm mesh of flake graphite, Mater. Lett., 60 (2006) 3927–3930.
[9] S.R. Dhakate, S. Sharma, M. Borah, R.B. Mathur, T.L. Dhami, Expanded graphite-based electrically conductive composites as bipolar plate for PEM fuel cell, Int. J. Hydrogen Energy, 33 (2008) 7146–7152.
[10] X. Creary, K. Chormanski, G. Peirats, C. Renneburg, Electronic properties of triazoles. Experimental and computational determination of carbocation and radical stabilizing properties, Polym. Compos., 33 (2012) 872–880.
[11] Y.P. Yao, Preparation of sulfur-free expanded graphite and its influencing factors, Lubr. Eng., 37 (2012) 90–92.
[12] J. Li, M. Li, Ultrasound irradiation prepare sulfur-free and lower exfoliate-temperature expandable graphite, Mater. Lett., 62 (2008) 2047–2049.
[13] M.S. Zhou, Y. Huang, Y. Tao, Preparation and expansion properties of a graphite intercalation compound containing phosphorus, Carbon, 98 (2016) 734–734.
[14] X. Lv, X. Wang, Z. Huang, C. Lv, Preparation of exfoliated graphite intercalated with nitrogen dioxide by direct gas phase processing, Mater. Lett., 136 (2014) 48–51.
[15] V. Sen, G.N. Demirer, Anaerobic treatment of real textile wastewater with a fluidized bed reactor, Water Res., 37 (2003) 1868–1878.
[16] M. Vilaseca, V. Lópezgrimau, C. Gutiérrezbouzán, Valorization of waste obtained from oil extraction in *Moringa oleifera* seeds: coagulation of reactive dyes in textile effluents, Materials, 7 (2014) 6569–6584.
[17] Z.X. Jing, X.F. Sun, Q. Ye, Y.J. Li, Hemicellulose-based porous hydrogel for methylene blue adsorption, Adv. Mater. Res., 560–561 (2012) 482–487.
[18] C. Saucier, M.A. Adebayo, E.C. Lima, R. Cataluña, P.S. Thue, L.D. Prola, M.J. Puchana-Rosero, F.M. Machado, F.A. Pavan, G.L. Dotto, Microwave-assisted activated carbon from cocoa shell as adsorbent for removal of sodium diclofenac and nimesulide from aqueous effluents, J. Hazard. Mater., 289 (2015) 18–27.
[19] J.H. Li, L.L. Feng, Z.X. Jia, Preparation of expanded graphite with 160 μm mesh of fine flake graphite, Mater. Lett., 60 (2006) 746–749.
[20] Z.R. Ying, X.M. Lin, Q. Yu, J. Luo, Preparation and characterization of low-temperature expandable graphite, Mater. Res. Bull., 43 (2008) 2677–2686.
[21] J. He, L.Z. Song, H.X. Yang, L.F. Xing, Preparation of sulfur-free exfoliated graphite by a two-step intercalation process and its application for adsorption of oils, J. Chem., 2017 (2017) 1–8.
[22] C. Tonin, A. Varesano, M. Canetti, W. Porzio, M. Catellani, Vapour phase polymerisation of pyrrole on cellulose-based textile substrates, Synth. Met., 156 (2006) 379–386.
[23] C. Zheng, X. Li, Q. Zhao, Z. Qu, X. Quan, Photo-oxidation of gas-phase cyclohexane species over nanostructured TiO_2 fabricated by different strategies, Sep. Purif. Technol., 67 (2009) 326–330.
[24] A.S. Orabi, A.M. Abbas, S.A. Sallam, Spectral, magnetic, thermal and DNA interaction of Ni (II) complexes of glutamic acid schiff bases, Synth. React. Inorg. Met.-Org. Chem., 43 (2013) 63–75.
[25] M. Mellado, A. Madrid, H. Peñacortés, R. López, C. Jara, Antioxidant activity of anthraquinones isolated from leaves of *Muehlenbeckia hastulata* (J.E. SM.) Johnst. (*Polygonaceae*), J. Chil. Chem. Soc., 58 (2013) 1767–1770.
[26] Z. Yan, X. Li, J. Huang, W. Xing, Z. Yan, Functionalization of petroleum coke-derived carbon for synergistically enhanced capacitive performance, Nanoscale Res. Lett., 11 (2016) 163.
[27] G. Vasuki, R. Selvaraju, Growth and characterization of uric acid crystals, Int. J. Sci. Res., 3 (2014) 2319–7064.
[28] A.C. Ferrari, J.C. Meyer, V. Scardaci, C. Casiraghi, M. Lazzeri, F. Mauri, Raman spectrum of graphene and graphene layers, Phys. Rev. Lett., 97 (2006) 187–401.
[29] Q. Zheng, Z. Cai, Z. Ma, S. Gong, Cellulose nanofibril/reduced graphene oxide/carbon nanotube hybrid aerogels for highly flexible and all-solid-state supercapacitors, ACS Appl. Mater. Interfaces, 7 (2015) 3263–3271.

[30] C. Tripisciano, S. Costa, R.J. Kalenczuk, E. Borowiak-Palen, Cisplatin filled multiwalled carbon nanotubes a novel molecular hybrid of anticancer drug container, Eur. Phys. J. B, 75 (2010) 141–146.
[31] S.J. Yang, J.H. Kang, H. Jung, T. Kim, C.R. Park, Preparation of a freestanding, macroporous reduced graphene oxide film as an efficient and recyclable sorbent for oils and organic solvents, J. Mater. Chem. A, 1 (2013) 9427–9432.
[32] X.F. Zhang, Z.X. Lu, J.Q. Zhao, Q.Y. Li, W. Zhang, C.H. Lu, Exfoliation/dispersion of low-temperature expandable graphite in nanocellulose matrix by wet co-milling, Carbohydr. Polym., 157 (2016) 1434–1441.
[33] L. Kőrösi, S. Papp, S. Beke, A. Oszkó, I. Dékány, Effects of phosphate modification on the structure and surface properties of ordered mesoporous SnO_2, Microporous Mesoporous Mater., 134 (2010) 79–86.
[34] K. Kan, L. Wang, P. Yu, J.J. Bao, K.Y. Shi, H.G. Fu, 2D quasi-ordered nitrogen-enriched porous carbon nanohybrids for high energy density supercapacitors, Nanoscale, 8 (2016) 10166–10176.
[35] S. Venkateswarlu, D. Lee, M. Yoon, Bioinspired 2D-carbon flakes and Fe_3O_4 nanoparticles composite for arsenite removal, ACS Appl. Mater. Interfaces, 8 (2016) 23876–23885.
[36] D.X. Yang, A. Velamakanni, G. Bozoklu, S. Park, M. Stoller, R.D. Piner, S. Stankovich, I. Jung, D.A. Field, C.A. Ventrice, R.S. Jr. Ruoff, Chemical analysis of graphene oxide films after heat and chemical treatments by X-ray photoelectron and Micro-Raman spectroscopy, Carbon, 47 (2009) 145–152.